

Wavepacket reconstruction via local dynamics in a parabolic lattice

Quentin Thommen, Véronique Zehnlé, and Jean Claude Garreau

Laboratoire de Physique des Lasers, Atomes et Molécules

Centre d'Etudes et de Recherches Laser et Applications,

Université des Sciences et Technologies de Lille,

*F-59655 Villeneuve d'Ascq Cedex, France**

(Dated: November 20, 2018)

We study the dynamics of a wavepacket in a potential formed by the sum of a periodic lattice and of a parabolic potential. The dynamics of the wavepacket is essentially a superposition of “local Bloch oscillations”, whose frequency is proportional to the local slope of the parabolic potential. We show that the amplitude and the phase of the Fourier transform of a signal characterizing this dynamics contains information about the amplitude and the phase of the wavepacket at a given lattice site. Hence, *complete* reconstruction of the the wavepacket in the real space can be performed from the study of the dynamics of the system.

PACS numbers: 03.65.-w, 03.75.-b, 32.80.Pj

The reconstruction of the wavefunction of a quantum system in the real space from experimentally accessible measurements is seldom possible. Even when the spatial probability distribution is accessible, phase measurements in general require the use of a completely different, and often incompatible, technique. This is essentially due to the fact that a measurement of the position of a quantum system is usually accompanied by a wavepacket reduction that erases the phase information. In a one-atom Magneto-optical trap [1] (prepared in a reproductive way), repeated measurements of the fluorescence light allow reconstruction of the atom probability distribution with a precision of the order of the wavelength of the detected light, whereas a measurement of wavepacket phases needs a specific atom-interferometry setup.

In contrast, the quantum dynamics of a system is highly sensitive to both the amplitude and the phase of the wavepacket. The idea at the root of the present letter is to use information on the dynamics of the system to determine simultaneously both these quantities, with a spatial resolution at least comparable to that of the methods mentioned in the preceding paragraph. The dynamics exploited here is related to the so-called “Bloch oscillation” (BO) observed in the motion of a quantum particle in a spatially periodic lattice to which a constant slope is added, forming a “tilted lattice”. In such a potential, instead of climbing down the slope of the potential, the wavepacket performs bounded periodic oscillations in real and momentum spaces. The origin of this oscillatory motion can be retraced to quantum interference among pieces of the original wave packet that are transmitted and reflected by the successive potential barriers of the lattice, in much analogy with a chain of optical interferometers with a linearly varying effective index [2]. The coherence of the wavepacket is thus a pre-requisite to the

observation of the BO. The frequency of oscillation (the “Bloch frequency”) corresponds to the energy shift from one lattice well to the next, and thus to the slope of the potential. This behavior, theoretically predicted in 1934 [3], has been observed experimentally in solid-state superlattices [4], with cold atoms [5], with Bose-Einstein condensates [6], and also with photons, in arrays of optical waveguides [2]. A theoretical study of the BO in an frame close to that adopted here can be found in Ref. [7].

Let us consider a quantum system, the “atom”, of mass M , placed in an one-dimensional potential formed by a spatially-periodic lattice of period d , to which a parabolic term $ax^2/2$ is added. With cold-atoms, this can be obtained by using a far-detuned standing wave which creates a sinusoidal lattice [5, 6, 8], superposed to an independent, focalized laser beam, producing a parabolic term (a laser-atom detuning much greater than the natural width of the concerned electronic transition reduces spontaneous emission, insuring the system to be conservative). The Hamiltonian of the system is

$$H = -\frac{1}{2M^*} \frac{\partial^2}{\partial x^2} - V_0 \cos(2\pi x) + \frac{x^2}{2} \quad (1)$$

where we introduced dimensionless units in which distances are measured in units of the lattice period d , energy is measured in units of ad^2 [or, equivalently, time is measured in units of $\hbar/(ad^2)$], $M^* \equiv Mad^4/\hbar^2$ is a reduced mass, and $\hbar = 1$. Without loss of generality, we shall use a sinusoidal lattice.

The energy spectrum of the Hamiltonian Eq. (1) is plotted in Fig. 1 and shows two distinct kinds of states. For energies below a threshold value ε_L , the corresponding eigenstates are localized in symmetric lattice wells $-n$ and n (where the lattice site at $n = 0$ is tied to the symmetry axis of the parabola). For each possible value of the energy, one finds a symmetric and an anti-symmetric quasi-degenerated states, which are noted resp. $\phi_n^S(x)$ and $\phi_n^A(x)$. We suppose that the depth of the lattice is such that there are only one symmetric and one anti-symmetric state for each couple of lattice wells n and $-n$

*URL: <http://www.phlam.univ-lille1.fr>

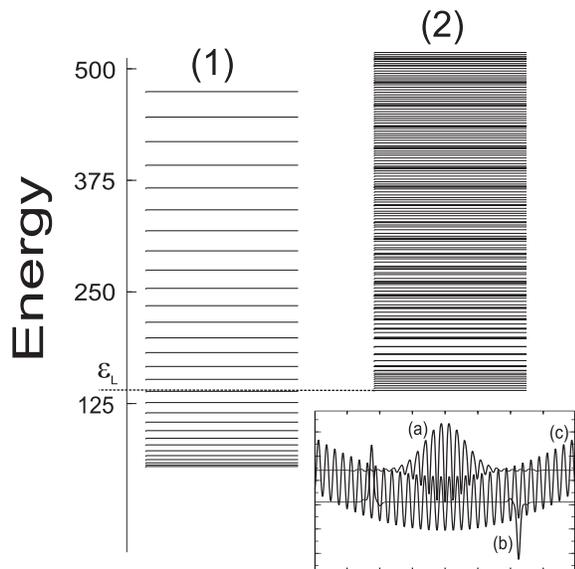


FIG. 1: Energy spectrum of the Hamiltonian Eq. (1). Column (1) represents the energies of localized states, with a parabolic distribution. Column (2) displays the energies of the delocalized states. The inset displays the wavefunction's modulus for a typical delocalized state (a), and a (anti-symmetric) localized state (b), compared to the parabolic lattice (c). $V_0 = 90$.

($V_0 = 90$). The corresponding eigenenergies are noted $n^2/2 + \delta_n^S$ and $n^2/2 + \delta_n^A$. For energies *above* ϵ_L , one finds both localized and delocalized states. At high energies, the latter are similar to the eigenstates of the harmonic oscillator and their eigenenergies approximately display a linear dependence on n (although this is not easily seen in Fig. 1).

We suppose that the atom wavepacket has been prepared in a superposition of *localized* states only. For high enough lattice amplitude V_0 , one can neglect the energy shifts δ_n^S and δ_n^A [9], and consider as a new basis the left and right quasi-eigenstates $\phi_{\pm n}(x) \equiv [\phi_n^S(x) \pm \phi_n^A(x)] / \sqrt{2}$, which are localized in the lattice site $\pm n$ with energy $\epsilon_n = n^2/2$ (up to an additive constant). Moreover, the localized eigenstates $\phi_n(x)$ are almost invariant under a translation by an integer number of steps of the lattice: $\phi_n(x) \approx \phi_m[x - (n - m)d]$. This property is exactly verified for a tilted lattice, and is a good approximation in the present problem as long as the parabolic potential do not perturb too much the translational invariance of the lattice wells over the spatial extension corresponding to the atom wavepacket (that is, as long as $V_0 \gg 1$ in our units).

At time $t = 0$ the wavepacket $\Psi_0(x)$ is centered at n_0 and has a spatial extension Δn : $\Psi_0 = \sum_n c_n \phi_n(x)$. At time t one has:

$$\Psi(x, t) = \sum_n c_n \exp\left[-i\frac{n^2}{2}t\right] \phi_n(x) \quad (2)$$

from which one can determine the dynamics of the system

[7]. For instance, the packet average position is

$$\bar{x} = \langle \Psi | x | \Psi \rangle = \sum_n X_m c_n c_{n-m}^* \exp\left[-im\left(n - \frac{m}{2}\right)t\right] \quad (3)$$

($X_m \equiv \langle \phi_n | x | \phi_{n+m} \rangle$ is almost independent of n).

Eq. (3) shows that, given the evolution of a quantum system, its coherences $c_n c_{n-m}^*$ can be obtained from the complex amplitude of the oscillations at the Bohr frequency ω_{nm} :

$$\omega_{nm} = \epsilon_n - \epsilon_m = m(n - m/2). \quad (4)$$

The parabolic component of the potential produces *non-degenerate* Bohr frequencies. In a tilted lattice corresponding to a constant force F , the coherences between neighbor sites $c_n c_{n-1}^*$ correspond to an oscillation with the *degenerate* (n -independent) Bohr (or Bloch) frequency $\omega_B = Fd/\hbar$ ($\omega_B = F$ in reduced units). The parabolic potential, on the contrary, has a local slope $F = x$ and the related “local” Bloch frequency depends on n . The local Bloch frequency (LBF) is by definition the Bohr frequency associated to neighbor sites at n and $n - 1$ ($m = 1$):

$$\omega_B(n) = \epsilon_n - \epsilon_{n-1} = n - \frac{1}{2}. \quad (5)$$

The presence of such a frequency in the dynamics is a signature of the coherence $c_n c_{n-1}^*$ that can be used to track the wavepacket amplitude and phase, as shown below.

Experimentally, it is more convenient to work in the momentum-representation, because the spatial amplitude of the BO is in general very small whereas, in the momentum space, the amplitude of the oscillation is of the order of \hbar/d (the extension of a Brillouin zone of the lattice), which is easy to resolve with available experimental methods. For cold atoms, for example, stimulated Raman transitions [10] can be used to that end. A great deal of information can be obtained by just monitoring the evolution of the probability for a given value p of the momentum, $P(p, t)$. We thus work in momentum space and introduce the eigenstates $\varphi_n(p)$ in p -representation:

$$\begin{aligned} \varphi_n(p) &\approx \frac{1}{\sqrt{2\pi}} \int \exp(ipx) \phi_{n_0}[x - (n - n_0)] dx \\ &= \exp[i(n - n_0)p] \varphi_{n_0}(p) \end{aligned} \quad (6)$$

where we used the approximate translation invariance of the real-space eigenfunctions $\phi_n(x)$. The evolution of the momentum probability-distribution is then:

$$\begin{aligned} P(p, t) &= |\Psi(p, t)|^2 = |\varphi_{n_0}(p)|^2 \times \\ &\left(1 + \sum_{m \neq 0} \exp(im p)\right) \\ &\sum_{n \neq m} c_n c_{n-m}^* \exp\left[-im\left(n - \frac{m}{2}\right)t\right] \end{aligned} \quad (7)$$

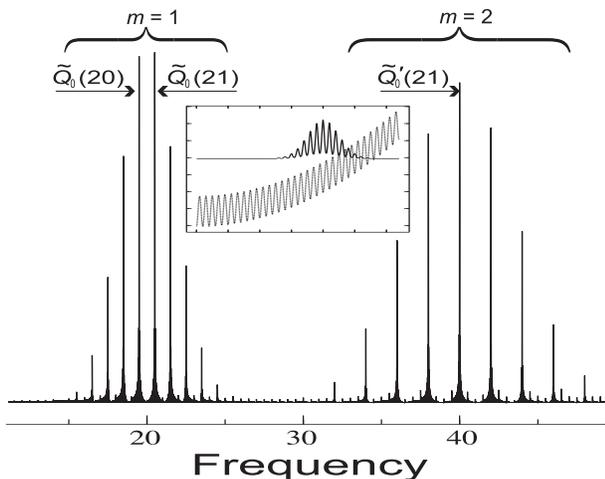


FIG. 2: Fourier transform of the probability of finding the system in the zero-momentum state, $P_0(t)$. The envelope of both frequency folds well reproduces the envelope of $|\Psi_0(x)|$ (see inset). The arrows indicate the components corresponding to the coherences between neighbor-sites $\tilde{Q}_0(n) = c_n c_{n-1}^*$ ($n = 20, 21$) and next-to-neighbor-sites $\tilde{Q}'_0(21) = c_{21} c_{19}^*$. $V_0 = 90$, $n_0 = 21$, and $\Delta n = 7$.

Fig. 2 displays the Fourier transform of the quantity $P_0(t) \equiv P(0, t)$ and has been obtained as follows. The time-dependent probability distribution $P_0(t)$ is calculated by numerical integration of the Schrödinger equation with the hamiltonian of Eq. (1) and with the initial wavepacket $\Psi_0(x)$ shown in the inset of Fig. 2 (the phase of c_n is arbitrarily set to $e^{in\pi/4}$). The spectrum of $P_0(t)$ presents components at the Bohr frequencies contained in Eq. (7), from which the amplitude and phase of the coherences $c_n c_{n-m}^*$ can be deduced. The interpretation of the spectrum may be complicated by the fact that Bohr frequencies corresponding to energy differences higher than next-neighbor wells may show up. These frequencies, corresponding to $m > 1$ in Eq. (4), are higher than the LBF [Eq. (5)] typically by a factor m . In the general case, the spectrum is thus composed of “folds” described by an integer value of m . However, a judicious choice of position of the wavepacket in the parabolic potential allow to separate one fold from the others. Frequency folds $m = 1$ and $m = 2$ are resolved if $n_0 + \Delta n/2 + 1/2 < 2(n_0 - \Delta n/2 - 1)$ or, roughly, $\Delta n \ll n_0$. In producing Fig. 2, we managed to satisfy this condition. The first frequency fold is clearly seen as the low-frequency part of the spectrum associated to the coherences $c_n c_{n-1}^*$. In Fig. 2, the shape of the wavepacket is reproduced by the envelopes of both the first and the second frequency folds. This is the case if the wavepacket is smooth enough at the scale of the lattice step that we can take $|c_n| \approx |c_{n-1}|$, and then directly identify the amplitude of the n -component of the spectrum with $|c_n|$.

The complete reconstruction of the spatial wavefunction from the c_n coefficients requires, in principle, the knowledge of the eigenstates of system. The detailed spa-

tial shape of the eigenstates may depend on experimental parameters that may not be known with a sufficient precision. With our system, the shape of the localized states is almost independent of n , as it is essentially determined by the lattice, the parabolic term giving a small correction. As they are sharply localized, they can be considered as delta-function-like, probing the local value of the wavepacket. The detailed shape of the eigenstates is thus not required for the reconstruction, at the a precision corresponding to a lattice step.

We can now proceed to the complete reconstruction of a wavepacket. We consider the first fold ($m = 1$) of the spectrum, and the zero momentum probability $P_0(t)$ only. The other folds have essentially the same structure; other values of the probed momentum may be used to extract complementary information or improve the accuracy of the reconstruction. We thus reduce Eq. (7) to the simpler form:

$$\begin{aligned} Q_0(t) &\equiv \frac{P_0(t)}{|\varphi_{n_0}(0)|^2} - 1 \\ &= \sum_n c_n c_{n-1}^* \exp \left[-i \left(n - \frac{1}{2} \right) t \right]. \end{aligned} \quad (8)$$

One then sees that the Fourier component $\tilde{Q}_0(n) = c_n c_{n-1}^*$ of Q_0 at frequency $n - 1/2$ directly gives the coherence between neighbor sites. If the wavepacket envelope is smooth, the amplitudes can be directly obtained by taking $|c_n|^2 \approx |\tilde{Q}_0(n)|$. If the phase also varies smoothly, the phase shift from the site $n - 1$ to the site n is also directly obtained from the phase of $\tilde{Q}_0(n)$, up to an unavoidable, but unimportant, global phase factor.

A more precise determination of the coefficients c_n is obtained by using the second frequency fold which, as one can easily convince oneself, gives the coherences $c_n c_{n-2}^* \equiv \tilde{Q}'_0(n)$, and the identity:

$$\frac{\tilde{Q}_0(n) \tilde{Q}_0(n+1)}{\tilde{Q}'_0(n+1)} = |c_n|^2. \quad (9)$$

The phase shifts can be straightforwardly obtained from the $\tilde{Q}_0(n)$. We display in Fig. 3 the coherences c_n deduced from the spectrum of Fig. 2. The agreement with the amplitudes of the original wavepacket is excellent. The figure also shows real and imaginary parts of the complex amplitudes in very good agreement with the original wavepacket.

We numerically verified that the above method can be applied to wavepackets of arbitrary shape. The reconstructed state then reproduces the wavepacket at the scale of the lattice step, all finer features are lost. A large number of delocalized states can appear in the decomposition of the initial state, but their contribution to the Bloch-oscillation spectrum is to add a wide background whose amplitude is much smaller than the peaks associated to the coherence between localized states.

Consider now the case in which there are many atoms simultaneously interacting with the potential. If the density of atoms is low, so that there is in average one atom

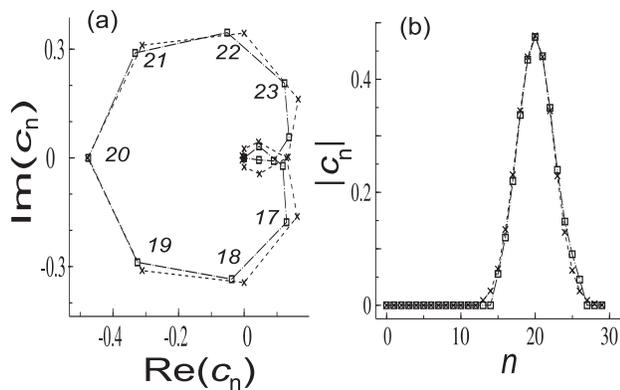


FIG. 3: Reconstruction of the initial wavepacket. Real and imaginary parts of c_n are shown in (a), evidencing the very good agreement between phases and amplitudes of the original wavepacket components (\times) and the reconstructed values (\square). The method correctly reproduces the phase mismatch between neighbors $\phi = \pi/4$. Curve (b) shows explicitly the amplitudes versus n and compares these values with the ones of the original wavepacket.

per site (or less), the present method reconstructs the atom distribution. If the atomic density is higher, the method measures the ensemble average of the atomic correlation $\langle c_n c_{n-m}^* \rangle$. This quantity is very important because it determines the ability of the system to display coherent quantum dynamics [7]. Finally, note that the present method can also be applied to a tridimensional lattice: adding a parabolic potential in a given direction of the lattice will probe the wavefunction along this direction.

In conclusion, we have presented a method allowing reconstruction of the spatial wavefunction of a quantum system using the Fourier spectrum of the Bloch oscil-

lations in a periodic lattice superposed to a parabolic potential. Our method is quite general: it does not depend, e.g. on internal properties of the quantum particle being studied, or on the shape of the lattice wells. A parabolic shape is not necessary provided that (i) the Bohr (or Bloch) frequencies of the system are not degenerated and (ii) the approximate translational symmetry of the localized states is preserved. The method requires a potential shape presenting both a non-constant and non-vanishing slope in the region of interest: the local slope induces local Bloch oscillation and the spatial dependence, in turn, leads to the position-sensitivity of the method. In principle, the method is applicable to a variety of systems, including cold atoms in light potentials, Bose-Einstein condensates and electrons in an adequately constructed superlattice. Applied to a Bose-Einstein condensate, whose Bloch oscillations have been recently observed [6], the present method may be used to probe nonlinear collective interactions. The method is also able to probe the *spatial entanglement* of two or more atoms, which can be of interest in the context of quantum information and quantum computing. We shall treat these interesting applications in the future.

The authors would like to acknowledge D. Delande, P. Szafranski and H. Lignier for fruitful discussions. This work is partially supported by an action “ACI Photonique” of the Ministère de la Recherche. Laboratoire de Physique des Lasers, Atomes et Molécules (PhLAM) is UMR 8523 du CNRS et de l’Université des Sciences et Technologies de Lille. Centre d’Etudes et Recherches Lasers et Applications (CERLA) is FR 2416 du CNRS, supported by Ministère de la Recherche, Région Nord-Pas de Calais and Fonds Européen de Développement Economique des Régions (FEDER).

-
- [1] Z. Hu and H. J. Kimble, *Opt. Lett.* **19**, 1888 (1994); F. Ruschewitz, D. Betterman, J. L. Peng, and W. Ertmer, *Europhys. Lett.* **34**, 651 (1996); D. Haubrich, H. Schadowinkel, F. Strauch, B. Überholtz, R. Wynands, and D. Meschede, *ibid.* **34**, 663 (1996).
 - [2] T. Pertsch, P. Dannberg, W. Elflein, A. Bräuer, and F. Lederer, *Phys. Rev. Lett.* **83**, 4752 (1999); R. Morandotti, U. Peschel, J. S. Aitchison, H. S. Eisenberg, and Y. Silberberg, *ibid.* **83**, 4756 (1999).
 - [3] C. Zener, *Proc. R. Soc. London, sect. A*, **145**, 243 (1934); a reprint can be found in *The Many-body problem*, D. C. Mattis Ed., World Scientific, Singapore, 1993.
 - [4] E. E. Mendez, F. Agulló-Rueda, and J. M. Hong, *Phys. Rev. Lett.* **60**, 2426 (1988); P. Voisin, J. Bleuse, C. Bouche, S. Gaillard, C. Alibert, and A. Regreny, *ibid.* **61**, 1639 (1988).
 - [5] M. Ben Dahan, E. Peik, J. Reichel, Y. Castin, and C. Salomon, *Phys. Rev. Lett.* **76**, 4508 (1996).
 - [6] O. Morsch, J. H. Müller, M. Cristiani, D. Ciampini, and E. Arimondo, *Phys. Rev. Lett.* **87**, 140402 (2001).
 - [7] Q. Thommen, J. C. Garreau, and V. Zehnlé, to appear in *Phys. Rev. A.*, preprint *arXiv:quant-ph/0112109*.
 - [8] S. R. Wilkinson, C. F. Bharucha, K. W. Madison, Q. Niu, and M. G. Raizen, *Phys. Rev. Lett.* **76**, 4512 (1996).
 - [9] The energy difference $|\delta_n^A - \delta_n^S|/n^2$ is typically of the order of 10^{-5} for $V_0 = 90$. Moreover, the $\delta_n^{A,S}$ are roughly independent of n .
 - [10] J. Ringot, P. Szafranski, J. C. Garreau, and D. Delande, *Phys. Rev. Lett.* **85**, 2741 (2000); J. Ringot, P. Szafranski, and J. C. Garreau, *Phys. Rev. A* **65**, 013403 (2002).